ChemPubSoc
Europe

❚ **Chemical Biology** |*Very Important Paper*|

VIP

A Chemical Proteomic Analysis of Illudin-Interacting Proteins

Philipp Le,[a] Matthew B. Nodwell,[a, b] Jürgen Eirich,[a, c] and Stephan A. Sieber*[a]

Abstract: The illudin natural product family are fungal secondary metabolites with a characteristic spirocyclopropyl-substituted fused 6,5-bicyclic ring system. They have been extensively studied for their cytotoxicity in various tumor cell types, and semisynthetic derivatives with improved therapeutic characteristics have progressed to clinical trials. Although it is believed that this potent alkylating compound class acts mainly through DNA modification, little is known about its binding to protein sites in a cellular context. To reveal putative protein targets of the illudin family in live cancer cells, we employed a semisynthetic strategy to access a series of illudin-based probes for activity-based protein profiling (ABPP). While the probes largely retained potent cytotoxicity, proteomic profiling studies unraveled multiple protein hits, suggesting that illudins exert their mode of action not from addressing a specific protein target but rather from DNA modification and unselective protein binding.

Introduction

The wealth of natural products represents a major source and inspiration for drug development.[1,2] Natural products exhibit diverse pharmacophores with a high degree of structural complexity, and, as a result of their co-evolution with living systems, they display a wide range of bioactivity. Fungal metabolism in particular has been found to be a rich source of valuable drug leads.

Illudins (Figure 1), a family of fungal sesquiterpenes first isolated from the poisonous Jack-o'-lantern mushroom *Omphalotus olearius* in the 1950s,[3–8] have been extensively studied for

Figure 1. Structures of illudin M and S and semisynthetic analogue irofulven (HMAF).

Illudin M, R = H
Illudin S, R = OH

Irofulven (HMAF)

[a] Dr. P. Le, Dr. M. B. Nodwell, Dr. J. Eirich, Prof. S. A. Sieber
Department Chemie, Center for Integrated Protein Science (CIPSM)
Technische Universität München, Lichtenbergstraße 4
85748 Garching (Germany)
E-mail: stephan.sieber@tum.de

[b] Dr. M. B. Nodwell
Current address: Department of Chemistry
Simon Fraser University, Burnaby (Canada)

[c] Dr. J. Eirich
Current address: Institute for Plant Biology and Biotechnology (IBBP)
Universität Münster, Münster (Germany)

Supporting information and the ORCID identification number(s) for the author(s) of this article can be found under:
https://doi.org/10.1002/chem.201902919.

their cytotoxicity in various tumor cell types. However, their poor selectivity for cancer cells versus normal cells and the resulting substantial systemic toxicity limited their effectiveness in animal models and restricted their potential use as anticancer agents.[9] Efforts to improve the therapeutic windows of this natural product class led to (semi)synthetic derivatives, including members of the acylfulvene compound class, which have been tested in various clinical trials for difficult-to-treat and multidrug resistant cancers.[10–12] The most promising acylfulvene analogue irofulven (6-hydroxymethylacylfulvene, HMAF; Figure 1)[13] progressed to phase III clinical trials against several cancer types before being terminated in 2012 because of lack of efficacy.[10, 14]

Illudins, in general, are thought to exert their biological effect mainly through DNA alkylation and DNA adduct formation, resulting in disruption of DNA synthesis/replication, cell arrest and induction of apoptosis.[9, 15, 16] The overall reactivity towards nucleophiles is facilitated by a unique activation mechanism to form electrophilic intermediates that react with bionucleophiles, such as DNA bases (Scheme 1). On a molecular basis, this two-step process is initiated by a Michael-type addition of a cellular nucleophile, such as thiols present in enzymes or glutathione, to form a electrophilic intermediate (**1**), followed by a second nucleophilic attack on the spirocyclopropyl group.[17–19] In addition to this, a metabolic reductive activation, the established activation mechanism of acylfulvenes,[20, 21] has been discussed for illudin S.[22–24] Here, enzymatic reduction of the carbon–carbon double bond of the α,β-unsaturated enone utilizing NADPH as cofactor leads to the formation of the biologically reactive electrophile (**4**). In both cases, the final nucleophilic opening of the spirocylcopropyl ring yields a stable aromatic product (**2**, **3**, **5** or **6**).

From the perspective of chemical reactivity, illudins readily react with thiol nucleophiles, such as cysteine and cysteine-containing peptides, at physiological pH in cell-free sys-
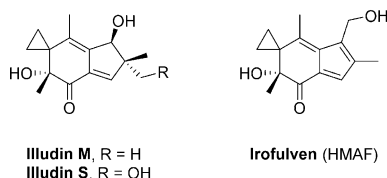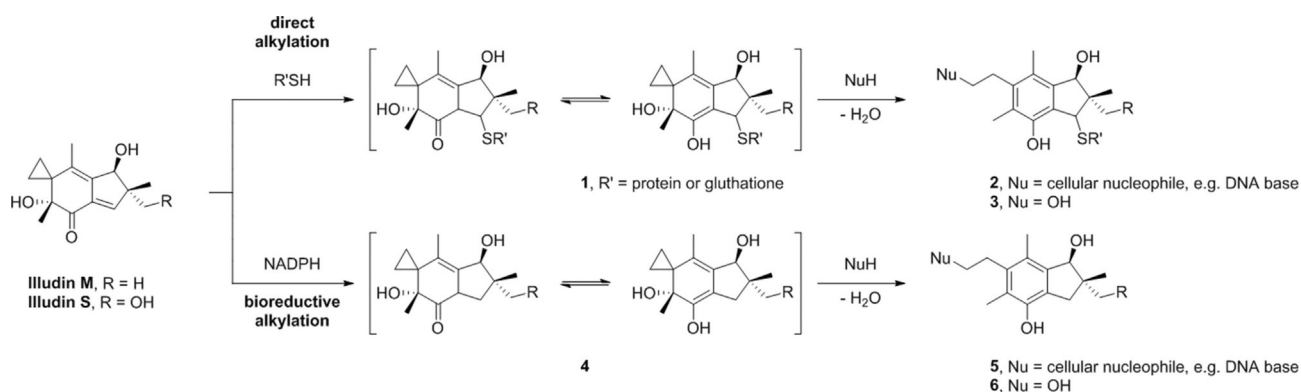
Scheme 1. Proposed mechanism for DNA alkylation involving conjugate addition to the α,β-unsaturated enone to form an electrophilic intermediate either through a cellular nucleophile (**1**) or thorough reductive bioactivation using NADPH for hydride delivery (**4**) followed by nucleophilic opening of the spirocyclopropyl ring to yield a stable aromatic product (**2**, **3**, **5**, or **6**).

tems.[18,25] Consequently, their chemical reactivity profile suggests alkylation of biological thiol nucleophiles present in enzymes as a possible cellular process that might contribute to their toxicity. For example, acylfulvene HMAF has been shown to display a large degree of protein reactivity,[26] and modification as well as inhibition of thiol-containing enzymes, including glutathione reductase and thioredoxin reductase, was reported for HMAF.[27,28] Analogous reactivity has been observed for the cyclopropyl-containing natural product duocarmycin, for which, in addition to DNA binding, the activated cyclopropyl ring reacts with nucleophilic protein active sites.[29]

To date, despite over 50 years of study, protein targets of the illudins remain obscure.[10] To uncover putative protein targets by proteomic profiling, we applied a semisynthetic strategy to isolate and modify illudin M and S for probe synthesis. These molecules were assayed for cytotoxicity against cancer cells and subsequently applied in activity-based protein profiling (ABPP). The list of targets suggests a global mode of protein reactivity matching the overall cytotoxic phenotype.

Results and Discussion

In line with its activation mechanism, previous structure–activity relationship (SAR) studies of illudins confirmed the primary enone-spirocyclopropyl pharmacophore as essential for cytotoxic activity.[19,30,31] Although the tertiary hydroxyl group seems to be vital for the unique reactivity of illudins, the primary hydroxyl group of illudin S is not crucial.[19] The free secondary hydroxyl group in the five-membered ring enhances cytotoxicity; however, esters of illudin M with largely retained cytotoxic effects have been reported.[32] These observations support the conclusion that the free primary and secondary hydroxyl groups act as putative sites for the introduction of a small terminal alkyne handle that is needed for proteomic profiling.

While multistep total syntheses of illudins are known,[33] we applied a semisynthetic approach to readily access illudin-based probes. Fermentation of *O. olearius* and isolation of illudin M (**ILM-0**) and S (**ILS-0**) was followed by their functionalization via synthetic chemistry. To this end, the illudin-producing

organism *O. olearius* was grown in a liquid-culture medium, the medium was extracted, and **ILM-0** and **ILS-0** were isolated by flash chromatography. Both natural products were synthetically equipped with alkyne handles by using various synthetic strategies (Figure 2): Esterification of **ILM-0** and **ILS-0** with 5-
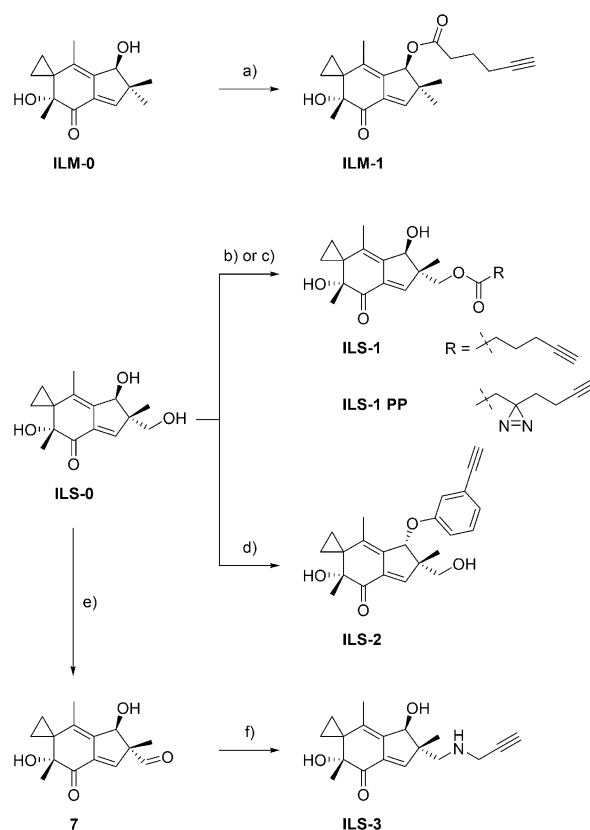

Figure 2. Semisynthetic strategy to access illudin-based ABPP probes: Isolation of natural products **ILM-0** and **ILS-0** from *O. olearius*, followed by introduction of terminal alkyne handles via synthetic chemistry to access illudin-based probes for proteomic profiling. Reaction conditions: a) 5-hexynoic acid, DIPC, CH$_2$Cl$_2$, RT, 24 h, 61%; b) 5-hexynoic acid, DIPC, DMAP, CH$_2$Cl$_2$, RT, 24 h, 55%; c) 2-(3-(but-3-yn-1-yl)-3*H*-diazirin-3-yl)acetic acid,[35] DIPC, DMAP, CH$_2$Cl$_2$, RT, 24 h, 65%; d) 3-ethynylphenol, PPh$_3$, DIAD, THF, RT, 24 h, 6%; e) PyrSO$_3$, DIPEA, DMSO, CH$_2$Cl$_2$, −20 °C, 1 h, 87%; f) i. propargylamine, Na$_2$SO$_4$, RT, 24 h; ii. NaBH(OAc)$_3$, RT, 16 h, 28%.

hexynoic acid gave access to the corresponding probes **ILM-1** and **ILS-1**. **ILS-0** was reacted with 3-ethynylphenol at its secondary hydroxyl group via a Mitsunobu-type reaction to yield probe **ILS-2**. Oxidation of **ILS-0** to the corresponding aldehyde **7** and subsequent reductive amination with propargylamine resulted in probe **ILS-3**. To account for reversible binding events, the natural product scaffold was equipped with a small terminal alkyne-containing diazirine photocrosslinking moiety[34] through esterification of **ILS-0** with 2-(3-(but-3-yn-1-yl)-3H-diazirin-3-yl) acetic acid[35] to yield photoprobe **ILS-1 PP**.

Prior to target identification via ABPP, we analyzed the effect of structural alterations caused by the introduction of the reporter tag on probe potency. To this end, illudin-based probes were tested against A549 lung cancer cells for cytotoxic effects. Whereas **ILM-1**, **ILS-1**, **ILS-1 PP**, and **ILS-3** displayed minimal loss of potency compared to the parent natural product, **ILS-2** showed a loss in activity by two orders of magnitude, reflecting the importance of the secondary hydroxyl group in illudin S activity (Table 1).

Table 1. Cytotoxicity (IC_{50}) of illudins and derived probes against A549 lung cancer cells (MTT assay, 24 h).[a]

	ILM-0	ILM-1	ILS-0	ILS-1	ILS-1 PP	ILS-2	ILS-3
IC50 [μM]	0.22	0.75	0.069	0.71	0.36	16.5[b]	0.75

[a] Data represent average values; $n = 3$ independent experiments in triplicate. [b] Data represents average value; $n = 2$ independent experiments in triplicate.

To visualize protein target binding in live cells via gel-based ABPP analysis (Figure 3 A), human cancer cells were incubated with illudin-based probes in varying concentrations. In case of

photoprobe **ILS-1 PP**, cells were subsequently irradiated with UV light. Following cell lysis, a fluorescence reporter group was introduced via copper(I)-catalyzed azide alkyne addition (CuAAC)[36–38] and proteins were separated via sodium dodecyl sulfate-polyacrylamide gel electrophoresis (SDS-PAGE). Fluorescence scanning revealed a panel of different protein bands, indicative of promiscuous protein labeling for each probe (Figures 3 B and S1–7). **ILS-3** as well as illudin M-based probe **ILM-1** did not display strong labeling at low micromolar concentrations in comparison to **ILS-1**, **ILS-2**, and **ILS-1 PP**.

To determine the identity of labeled proteins, we performed gel-free ABPP with quantification based on stable isotope labeling by amino acids in cell culture (SILAC; Figure 3 A). Based on the intense labeling profiles obtained on gels, **ILS-1**, **ILS-2**, and **ILS-1 PP** were selected for these studies. SILAC-cultured A549 cells were treated with probes, UV irradiated (only for **ILS-1 PP**) and lysed. Subsequently, probe-labeled proteins were ligated to biotin-PEG-N_3 via CuAAC, enriched on avidin beads, enzymatically digested, and the peptides were analyzed by gel-free, quantitative LC-MS/MS (Figures 4 and S8; Supporting Table in the Supporting Information).

Overlap of enriched proteins between the illudin-based probes (Figure 4 B, C) was generally low in the soluble fraction, with a total of four proteins being labeled by both **ILS-1** and **ILS-1 PP** (NPC1, RPS7, HMOX1, KRT18) as well as three proteins being labeled by **ILS-1 PP** and **ILS-2** (CTSD, ALDH1B1, PCYOX1). Interestingly, there were no enriched proteins shared among all three probes. The rather low cytotoxic activity of **ILS-2** might explain the overall low protein labeling profile of this probe because modification by the alkyne handle might have altered the affinity and specificity of **ILS-2** for the natural targets of illudins. GO term analysis revealed that some of the proteins enriched by **ILS-1** can be linked to nucleotide and/or
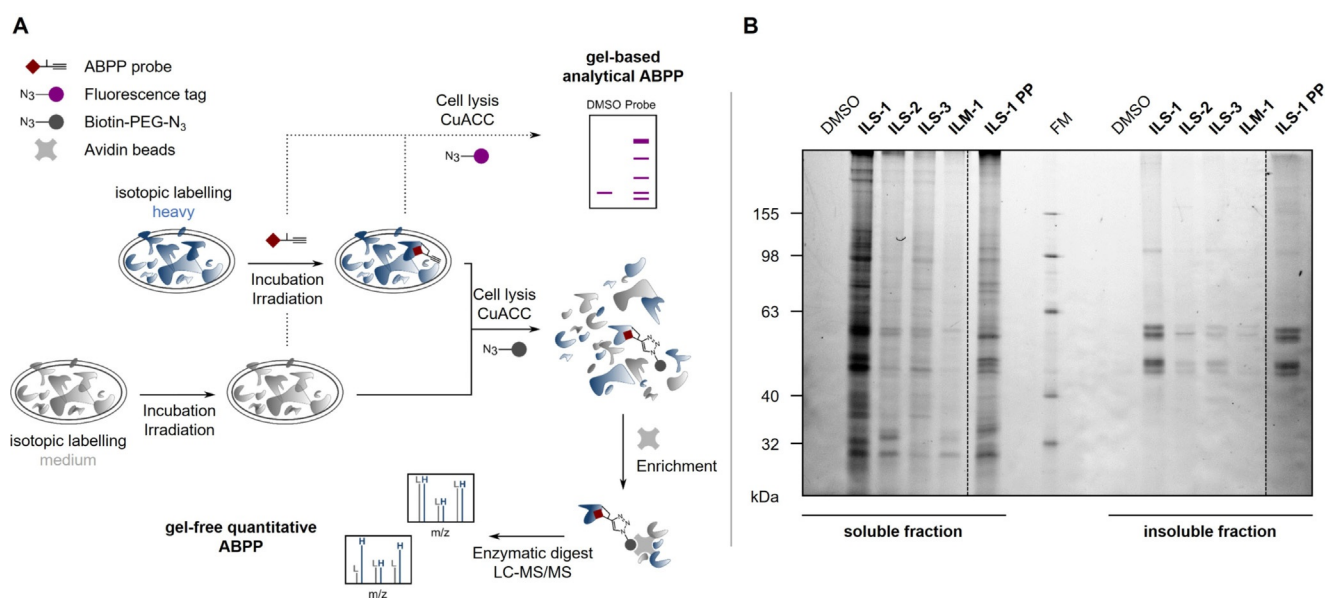

Figure 3. A) The concept of ABPP: Live cells are treated with probes, followed by optional UV irradiation. Cells are lysed, terminal alkynes functionalized with a reporter group by CuAAC and probe-labeled proteins visualized via fluorescence SDS-PAGE or identified via mass spectrometry-based proteomics after downstream protein enrichment. B) Analysis of protein binding: In-gel fluorescence analysis after labeling with **ILS-1**, **ILS-2**, **ILS-3**, **ILM-1**, and **ILS-1 PP** (10 μM; 1 h) in A549 cells. For Coomassie stained gel, see Figure S1.
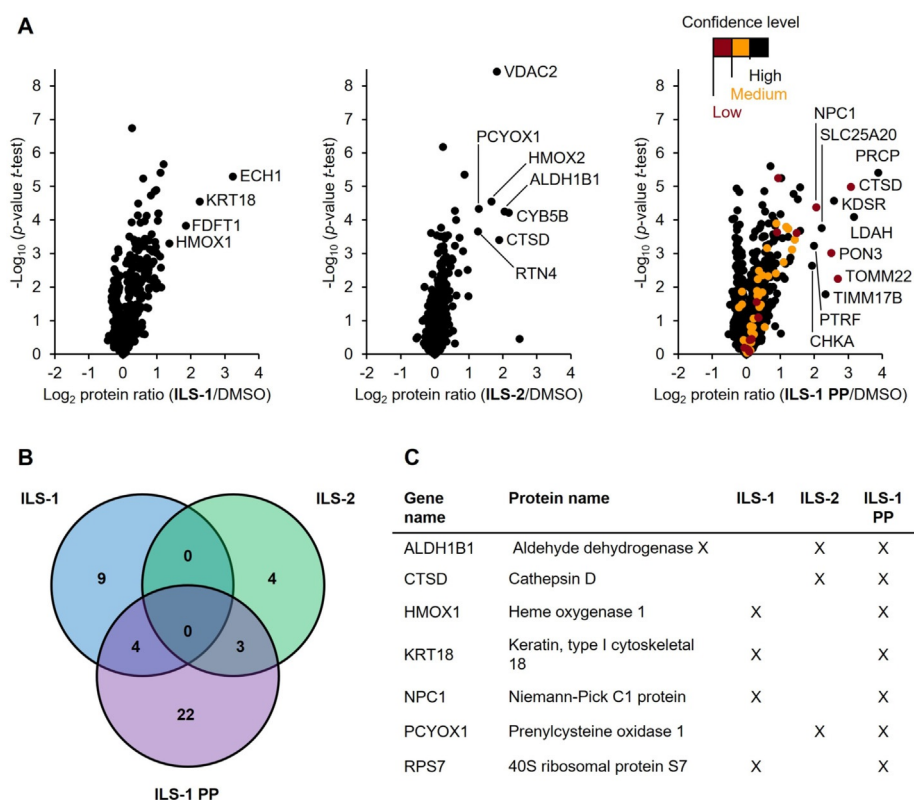
Figure 4. A) Protein labeling profiles of illudin-based probes **ILS-1**, **ILS-2**, and **ILS-1 PP** (3 μM; incubation for 1 h 37 °C; in case of **ILS-1 PP**, UV irradiation for 30 min, 4 °C) in A549 cells. Volcano plots illustrate the log$_2$-fold enrichment of proteins compared to DMSO in the soluble fraction. Identified proteins were aligned with diazirine-associated off-target protein binding published by Kleiner et al.[35] and classified accordingly as low-confidence (red), medium-confidence (yellow), or high-confidence (black) hits. Data represent average values; $n = 6$ (two independent experiments performed in triplicate). For protein labeling profiles of insoluble proteins, see Figure S8. For details, see the Supporting Table in the Supporting Information. B) Overlap of proteins identified in the **ILS-1**, **ILS-2**, and **ILS-1 PP** enrichment (log$_2$ protein ratio ≥ 1, $p \leq 0.05$). C) List of proteins enriched (log$_2$ protein ratio ≥ 1, $p \leq 0.05$) and shared by **ILS-1**, **ILS-2**, or **ILS-1 PP**.

DNA/RNA binding (see the Supporting Table in the Supporting Information). The majority of **ILS-1**, **ILS-2**, and **ILS-1 PP** labeled proteins however is of diverse functionality. While no proteins were enriched in the insoluble fraction of samples treated with **ILS-2** and **ILS-1 PP**, again various **ILS-1** labeled proteins can be linked to nucleotide and/or DNA/RNA binding by GO term analysis, including histones and splicing factors (Figure S8, Supporting Table in the Supporting Information). Overall, a closer inspection of the protein hits indicates a rather promiscuous labeling without clear preference for predominant targets in line with the gel-based data. In addition, most of the hits could not be connected with a toxic phenotype. We thus assume that illudins impact cell viability primarily by DNA modification rather than by protein modification. However, it is intriguing to speculate that the identification of DNA/RNA binding proteins as ABPP hits could reflect the dual reactivity of illudins, leading to crosslinking between nucleotides and interacting proteins in close proximity.

Conclusions

We employed a semisynthetic strategy to access illudin-based probes for a chemical proteomics approach to identify putative protein binding partners in complex proteomes of live cells.

Isolation of illudin M and S from *O. olearius* and subsequent synthetic modification of the natural product scaffold enabled the synthesis of several probes, which largely retained the potent cytotoxicity of the parent natural products. Subsequent quantitative chemical proteomic profiling in live cells identified a broad array of potential hits, including several nucleotide binding proteins. The large number of proteins lacking a clear toxic phenotype suggests that DNA binding, an already known target of illudins, predominantly contributes to cytotoxicity. We thus conclude that illudins exert their mode of action not from addressing a specific protein target but rather from DNA modification and unselective protein binding.

Experimental Section

General remarks

Reagents and solvents were purchased from commercial suppliers and used as received. Ultrapure water (H$_2$O$_{dd}$) was generated with a Milli-Q water purifier (Merck). All reactions involving air- and/or water-sensitive chemicals were carried out in oven-dried flasks under an argon atmosphere. Flash chromatography was performed on silica gel 60 (0.035–0.070 mm, mesh 60 Å, Merck). ^{1}H and proton-decoupled ^{13}C NMR spectra were recorded with a Bruker Avance III HD 300 (300 MHz), a Bruker Avance I 360 (360 MHz), a

Bruker Avance III HD (500 MHz), or a Bruker Avance III HD (500 MHz, equipped with a Bruker CryoProbe platform) at 298 K. Chemical shifts (δ) are referenced to the residual proton and carbon signals of the deuterated solvent. HRMS spectra were recorded in the ESI or APCI mode with a Thermo Fisher Scientific LTQ-FT Ultra (FT-ICR-MS) coupled with an UltiMate 3000 HPLC system (Thermo Fisher Scientific) or in the electron ionization (EI, 70 eV) mode with a Thermo Fisher Scientific DFS-HRMS spectrometer.

A549 cells were cultured in Dulbecco's Modified Eagle Medium (DMEM high glucose, 4.5 g L^{-1}; Life Technologies) supplemented with 10% fetal bovine serum (FBS; Sigma Life Science) and 2 mM L-glutamine (PAA). For SILAC-based experiments, A549 cells were passaged at least six times in SILAC-DMEM (Life Technologies) supplemented with 10% dialyzed FBS (Sigma Life Science) and 2 mM L-glutamine (PAA) as well as [$^{13}C_6$,$^{15}N_4$] L-arginine·HCl (214 μM) and [$^{13}C_6$,$^{15}N_2$] L-lysine·2 HCl (419 μM; Cambridge Isotope Laboratories) resulting in "heavy" cells or [$^{13}C_6$] L-arginine·HCl and [4,4,5,5-D$_4$] L-lysine·2 HCl (Cambridge Isotope Laboratories) in corresponding molarities resulting in "medium" cells. Cells were maintained at 37 °C in a humidified 5% CO$_2$ atmosphere and trypsin-EDTA was used for detachment of cells.

Isolation of ILM-0 and ILS-0

Mycelia from *Omphalotus olearius* CBS 102283 were cultured in sterile Czapek-Dox mineral broth (1 L) containing beechwood chips (ca. 60% w/v). After 30 days, a point at which the mycelial mats had covered the culture surface, the culture medium was extracted with EtOAc (3×800 mL). The combined organic phase was dried over Na$_2$SO$_4$, filtered, and the solvent removed. Purification of the resulting residue by flash column chromatography on silica (Hex/EtOAc 9:1 to 1:9) yielded **ILS-0** (168 mg, 0.636 mmol) and **ILM-0** (46.9 mg, 0.189 mmol).

ILM-0: R_f = 0.11 (Hex/EtOAc 4:1); ^{1}H NMR (500 MHz, CDCl$_3$): δ = 6.53 (s, 1H), 4.39 (s, 1H), 1.68 (s, 3H), 1.35 (s, 3H), 1.20 (s, 3H), 1.14–1.11 (m, 1H), 1.10 (s, 3H), 0.98–0.92 (m, 1H), 0.85–0.80 (m, 1H), 0.43–0.38 ppm (m, 1H); ^{13}C NMR (126 MHz, CDCl$_3$): δ = 200.6, 146.8, 138.9, 134.7, 133.1, 79.0, 76.1, 49.2, 31.7, 27.4, 24.9, 20.6, 14.4, 8.8, 6.1 ppm; EI-HRMS: m/z calcd for C$_{15}$H$_{20}$O$_3$$^+$: 248.1412 [M]$^+$; found: 248.1411.

ILS-0: R_f = 0.14 (Hex/EtOAc 2:3); ^{1}H NMR (500 MHz, CDCl$_3$): δ = 6.45 (s, 1H), 4.72 (s, 1H), 3.54 (d, J = 10.7 Hz, 2H), 3.47 (d, J = 10.7 Hz, 1H), 1.68 (s, 3H), 1.37 (s, 3H), 1.20 (s, 3H), 1.14–1.09 (m, 1H), 0.98–0.93 (m, 1H), 0.86–0.81 (m, 1H), 0.44–0.39 ppm (m, 1H); ^{13}C NMR (126 MHz, CDCl$_3$): δ = 200.6, 141.7, 138.6, 136.2, 135.2, 76.3, 75.0, 69.1, 55.2, 32.0, 24.9, 16.0, 14.3, 8.9, 6.2 ppm; EI-HRMS: m/z calcd for C$_{15}$H$_{20}$O$_4$$^+$: 264.1362 [M]$^+$; found: 264.1354.

Synthesis and characterization

Synthesis of ILM-1: **ILM-0** (25.0 mg, 0.101 mmol, 1.0 equiv.) and 5-hexynoic acid (13.3 μL, 13.6 mg, 0.121 mmol, 1.2 equiv.) were dissolved in CH$_2$Cl$_2$ (0.6 mL). N,N′-Diisopropylcarbodiimide (DIPC; 18.9 μL, 15.3 mg, 0.121 mmol, 1.2 equiv.) was added and the resulting solution was stirred at RT for 24 h. The solvents were removed and the resulting residue was purified by flash column chromatography on silica (Hex/EtOAc 9:1) to yield **ILM-1** (20.0 mg, 0.0616 mmol, 61%). R_f = 0.42 (Hex/EtOAc 1:1); ^{1}H NMR (500 MHz, CDCl$_3$): δ = 6.51 (s, 1H), 5.66 (s, 1H), 3.55 (s, 1H), 2.49 (td, J = 7.3, 1.7 Hz, 2H), 2.27 (td, J = 6.9, 2.6 Hz, 2H), 1.96 (t, J = 2.6 Hz, 1H), 1.86 (p, J = 7.2 Hz, 2H), 1.51 (s, 3H), 1.36 (s, 3H), 1.19 (s, 3H), 1.15–1.10 (m, 1H), 1.08 (s, 3H), 0.96–0.90 (m, 1H), 0.87–0.81 (m, 1H), 0.44–

0.37 ppm (m, 1H); ^{13}C NMR (75 MHz, CDCl$_3$): δ = 200.2, 172.9, 146.4, 135.6, 135.3, 133.7, 83.1, 79.0, 76.2, 69.4, 49.0, 32.9, 31.6, 26.9, 24.9, 23.8, 20.8, 18.0, 14.7, 9.0, 6.2 ppm; EI-HRMS: m/z calcd for C$_{21}$H$_{26}$O$_5$$^+$: 342.1831 [M]$^+$; found: 342.1826.

Synthesis of ILS-1: **ILS-0** (20.0 mg, 0.0757 mmol, 1.0 equiv.) and 5-hexynoic acid (8.32 μL, 8.49 mg, 0.0757 mmol, 1.0 equiv.) were dissolved in CH$_2$Cl$_2$ (0.5 mL). DIPC (11.8 μL, 9.55 mg, 0.0757 mmol, 1.0 equiv.) and 4-(dimethylamino)pyridine (DMAP; 9.25 mg, 0.0757 mmol, 1.0 equiv.) were added, and the resulting reaction mixture was stirred at RT for 24 h. The solvents were removed and the resulting residue was purified by flash column chromatography on silica (Hex/EtOAc 1:1) to yield **ILS-1** (15.0 mg, 0.0418 mmol, 55%). R_f = 0.70 (Hex/EtOAc 2:3); ^{1}H NMR (360 MHz, CDCl$_3$): δ = 6.45 (s, 1H), 4.61 (s, 1H), 3.97 (s, 2H), 3.53 (s, 1H), 2.44 (t, J = 7.4 Hz, 2H), 2.24 (td, J = 6.9, 2.6 Hz, 2H), 1.97 (t, J = 2.6 Hz, 1H), 1.80 (p, J = 7.1 Hz, 2H), 1.69 (s, 3H), 1.36 (s, 3H), 1.23 (s, 3H), 1.17–1.10 (m, 1H), 1.01–0.93 (m, 1H), 0.90–0.81 (m, 2H), 0.47–0.38 ppm (m, 1H); ^{13}C NMR (91 MHz, CDCl$_3$): δ = 200.2, 173.0, 140.9, 138.4, 135.9, 135.6, 83.2, 76.2, 75.2, 69.5, 69.4, 53.2, 32.9, 31.9, 24.9, 23.6, 18.0, 16.3, 14.3, 9.0, 6.2 ppm; EI-HRMS: m/z calcd for C$_{21}$H$_{26}$O$_5$$^+$: 358.1780 [M]$^+$; found: 358.1775.

Synthesis of ILS-1 PP: **ILS-0** (17.4 mg, 0.0658 mmol, 1.0 equiv.) and 2-(3-(but-3-yn-1-yl)-3H-diazirin-3-yl)acetic acid[35] (10.0 mg, 0.0658 mmol, 1.0 equiv.) were dissolved in CH$_2$Cl$_2$ (4 mL). DIPC (10.2 μL, 8.30 mg, 0.0658 mmol, 1.0 equiv.) and DMAP (8.04 mg, 0.0658 mmol, 1.0 equiv.) were added, and the resulting reaction mixture was stirred at RT for 16 h. The solvents were removed and the resulting residue was purified by flash column chromatography on silica (Hex/EtOAc 4:1) to yield **ILS-1 PP** (17.0 mg, 0.0427 mmol, 65%). R_f = 0.42 (Hex/EtOAc 1:1); ^{1}H NMR (500 MHz, CDCl$_3$): δ = 6.45 (s, 1H), 4.67 (s, 1H), 4.02 (s, 2H), 3.54 (s, 1H), 2.34 (s, 2H), 2.04 (td, J = 7.3, 2.8 Hz, 2H), 2.02–2.00 (m, 1H), 1.72 (td, J = 7.3, 1.3 Hz, 2H), 1.70 (s, 3H), 1.36 (s, 3H), 1.25 (s, 3H), 1.15–1.12 (m, 1H), 0.99–0.95 (m, 1H), 0.87–0.82 (m, 1H), 0.44–0.38 ppm (m, 1H); ^{13}C NMR (126 MHz, CDCl$_3$): δ = 200.3, 169.0, 140.3, 138.1, 136.1, 135.9, 82.5, 76.2, 75.1, 70.2, 69.7, 53.1, 39.8, 32.1, 32.0, 25.6, 24.9, 16.5, 14.3, 13.4, 9.0, 6.2 ppm; EI-HRMS: m/z calcd for C$_{22}$H$_{26}$N$_2$O$_5$$^+$: 398.1842 [M]$^+$; found: 398.1836.

Synthesis of ILS-2: **ILS-0** (40.0 mg, 0.151 mmol, 1.1 equiv.) and 3-ethynylphenol (16.2 mg, 0.137 mmol, 1.0 equiv.) were dissolved in THF (1 mL). Triphenylphosphine (PPh$_3$; 43.1 mg, 0.164 mmol, 1.2 equiv.) and diisopropyl azodicarboxylate (DIAD; 35.0 μL, 36.0 mg, 0.178 mmol, 1.3 equiv.) were added, and the resulting reaction mixture was stirred at RT for 24 h. The solvents were removed and the resulting residue was purified by flash column chromatography on silica (Hex/EtOAc 4:1) to yield **ILS-2** (3.2 mg, 0.00878 mmol, 6%). R_f = 0.78 (Hex/EtOAc 1:1); ^{1}H NMR (360 MHz, CDCl$_3$): δ = 7.30–7.24 (m, 1H), 7.18–7.10 (m, 2H), 7.03–6.97 (m, 1H), 6.61 (s, 1H), 5.29 (s, 1H), 3.82–3.62 (m, 2H), 3.60 (s, 1H), 3.09 (s, 1H), 2.04 (s, 1H), 1.38 (s, 3H), 1.32 (s, 3H), 1.28 (s, 3H), 1.22–1.14 (m, 1H), 0.99–0.91 (m, 1H), 0.88–0.79 (m, 1H), 0.49–0.41 ppm (m, 1H); ^{13}C NMR (91 MHz, CDCl$_3$): δ = 199.8, 158.2, 142.5, 142.4, 136.3, 135.7, 130.1, 126.2, 123.8, 119.5, 117.2, 85.6, 83.2, 77.9, 76.4, 66.4, 55.2, 32.7, 25.1, 22.7, 15.0, 9.5, 6.1 ppm; EI-HRMS: m/z calcd for C$_{23}$H$_{24}$O$_4$$^+$: 364.1675 [M]$^+$; found: 364.1658.

Synthesis of 7: **ILS-0** (32.4 mg, 0.123 mmol, 1.0 equiv.) was dissolved in CH$_2$Cl$_2$ (0.8 mL). N,N-Diisopropylethylamine (DIPEA; 85.9 μL, 63.6 mg, 0.492 mmol, 4.0 equiv.) was added and the resulting pale-yellow solution was cooled to −20 °C. A solution of sulfur trioxide pyridine complex (PyrSO$_3$; 78.3 mg, 0.492 mmol, 4.0 equiv.) in DMSO (0.8 mL) was added and the solution was stirred at −20 °C for 15 min. The reaction was quenched cold by the addition of H$_2$O (1 mL) and EtOAc (1 mL). The aqueous layer was saturated

with NaCl and extracted with EtOAc (2×5 mL). The combined organic phase was dried over Na_2SO_4, filtered and concentrated. The resulting residue was purified by flash column chromatography on silica (CH_2Cl_2/MeOH 95:5) to yield illudinal **7** (28.0 mg, 0.107 mmol, 87%). $R_f = 0.38$ (CH_2Cl_2/MeOH 95:5); ^1H NMR (360 MHz, CDCl$_3$): $\delta =$ 9.45 (s, 1H), 6.43 (s, 1H), 5.09 (s, 1H), 3.50 (s, 1H), 1.72 (s, 3H), 1.38 (s, 3H), 1.38 (s, 3H), 1.20–1.11 (m, 1H), 1.03–0.95 (m, 1H), 0.92–0.82 (m, 1H), 0.49–0.40 ppm (m, 1H); ^{13}C NMR (91 MHz, CDCl$_3$): $\delta =$ 199.9, 198.8, 137.8, 137.7, 137.6, 135.3, 76.4, 72.3, 65.4, 32.2, 24.9, 14.5, 14.0, 9.3, 6.4 ppm; EI-HRMS: m/z calcd for $C_{15}H_{18}O_4^+$: 262.1205 $[M]^+$; found: 262.1199.

Synthesis of ILS-3: Compound **7** (6.30 mg, 24.0 μmmol, 1.0 equiv.) was dissolved in THF (0.5 mL). Na_2SO_4 (54.5 mg, 0.384 mmol, 16 equiv.) and propargylamine (1.67 μL, 1.45 mg, 26.4 μmol, 1.1 equiv.) were added and the reaction mixture was stirred at RT for 24 h. $NaBH(OAc)_3$ (30.5 mg, 0.144 mmol, 6.0 equiv.) was added and the resulting mixture was stirred at RT overnight. The reaction was quenched with aqueous K_2CO_3 (1 mL) and the aqueous layer was extracted with EtOAc (2×2 mL). The combined organic phase was dried over Na_2SO_4, filtered and concentrated. The resulting residue was purified by flash column chromatography on silica (Hex/EtOAc 2:3) to yield **ILS-3** (2.00 mg, 6.64 μmol, 28%). $R_f = 0.12$ (Hex/EtOAc 2:3); ^1H NMR (500 MHz, CDCl$_3$): $\delta = 6.48$ (s, 1H), 4.75 (s, 1H), 3.41 (s, 2H), 2.74–2.60 (m, 3H), 2.22 (t, $J = 2.4$ Hz, 1H), 1.68 (s, 3H), 1.36 (s, 3H), 1.18 (s, 3H), 1.14–1.09 (m, 1H), 0.99–0.93 (m, 1H), 0.84–0.79 (m, 1H), 0.46–0.39 ppm (m, 1H); ^{13}C NMR (126 MHz, CDCl$_3$): $\delta = 200.7$, 142.9, 138.4, 135.4, 134.7, 82.0, 76.3, 76.2, 71.8, 57.0, 41.1, 39.0, 32.1, 25.0, 17.8, 14.2, 8.8, 6.1 ppm; ESI-HRMS: m/z calcd for $C_{18}H_{24}NO_3^+$: 302.1751 $[M + H]^+$; found: 302.1751.

Cytotoxicity assay (MTT)

A549 cells at 30–40% confluence were treated (37°C, humidified 5% CO_2 atmosphere, 24 h) with the test compound or DMSO in full growth media (100 μL/well, final concentration of DMSO 0.1%). Subsequently, thiazolyl blue tetrazolium bromide (20 μL; 5 mg mL^{-1} in PBS) was added, followed by incubation (37°C, humidified 5% CO_2 atmosphere) for 4 h. After removal of the medium, the resulting formazan was dissolved in DMSO (200 μL). Optical density was measured at 570 nm (562 nm) with background subtraction at 630 nm (620 nm) with a TECAN Infinite M200 Pro. MTT data were obtained from at least three independent experiments with triplicate runs. All measured values were normalized to values resulting from DMSO-treated samples (100% cell viability). IC_{50} values and 95% confidence intervals were calculated across all replicates.

Analytical in situ ABPP

A549 cells at 90% confluence (Nunc 6-well plate; Thermo Fisher Scientific) were treated (37°C, 5% CO_2, 1 h) with probe in PBS (1 mL; final concentration of DMSO 0.1%). For **ILS-1 PP** experiments, cells were irradiated with UV light (Philips TL-D 18W BLB, 360 nm maximum, 4°C, 30 min), prior to detachment by cell scraping and cell lysis (100 μL lysis buffer; 1% v/v NP40 and 1% w/v sodium deoxycholate in PBS; 4°C, 15 min). Following separation of soluble and insoluble fraction by centrifugation (20,000×g, 4°C, 15 min) and resuspension of the insoluble fraction in PBS (sonication at 10% intensity, 15 s), labeled proteins of both fractions (each 88 μL) were reacted via CuAAC (0.20 mM rhodamine-azide, 1.0 mM TCEP, 0.10 mM TBTA ligand and 1.0 mM $CuSO_4$; RT, 1 h). For protein separation by SDS gel electrophoresis, samples were diluted with 2× sample loading buffer (100 μL; 1:1 v/v; SLB: 32 mM Tris pH 6.8, 5% glycerol, 1% w/v SDS, 0.0013% w/v bromophenol blue, 2.5%

v/v 2-mercaptoethanol) and BenchMark Fluorescent Protein Standard (Invitrogen) was used. Fluorescence was recorded using a Fujifilm LAS 4000 luminescent image analyzer with a Fujinon VRF43LMD3 lens and a 575DF20 filter.

Preparative in situ ABPP

Isotopically labeled A549 cells (SILAC) at 90% confluence (15 cm dishes; Sarstedt) were treated (37°C, 5% CO_2, 1 h) with probe (3 μM) or DMSO in PBS (10 mL; final concentration of DMSO 0.1%). Isotopic labels were switched for replicate experiments. For **ILS-1 PP** experiments, cells were irradiated with UV light (Philips TL-D 18W BLB, 360 nm maximum, 4°C, 30 min), prior to detachment by cell scraping and cell lysis (1 mL lysis buffer; 1% v/v NP40 and 1% w/v sodium deoxycholate in PBS; 4°C, 15 min). Following separation of soluble and insoluble fraction by centrifugation (20000×g, 4°C, 15 min) and resuspension of the insoluble fraction in PBS (sonication at 10% intensity, 15 s), protein concentration was measured by BCA assay and equal protein amounts resulting from probe- and DMSO-treated samples of the oppose isotopic label were pooled. Labeled proteins of both fractions (each 1880 μL) were reacted via CuAAC (0.20 mM azide-PEG$_3$-biotin conjugate, 0.52 mM TCEP, 0.050 mM TBTA ligand and 0.50 mM $CuSO_4$; RT, 1 h), followed by precipitation with ice-cold acetone (8 mL; −20°C, 18 h). Proteins were collected by centrifugation (16900×g, 4°C, 15 min), washed with ice-cold methanol (2×1 mL) and resuspended in 0.2% w/v SDS in PBS (0.5 mL; sonication at 10% intensity, 15 s). Affinity enrichment (RT, 1 h) was performed with avidin agarose resin (Sigma, pre-washed with 0.4% w/v SDS in PBS (3× 1 mL); typically 50 μL of bead slurry was used for enrichment). Beads were thoroughly washed following pull-down (1 mL each time): 3×0.4% w/v SDS in PBS, 2×6 M urea in H_2O_{dd} and 3×PBS. Avidin agarose beads with bound proteins were resuspended in denaturation buffer (200 μL; 7 M urea, 2 M thiourea in 20 mM HEPES buffer, pH 7.5), followed by reduction with dithiothreitol (DTT; 1 mM; 37°C, 45 min), alkylation using iodoacetamide (IAA, 5.5 mM; 25°C, 30 min) and treatment with DTT (4 mM; 25°C, 30 min). Enzymatic digestion using Lys-C (2.5 ng μL^{-1}, MS-grade; Wako) was carried out at RT for 2 h, upon which samples were diluted with triethylammonium bicarbonate buffer (TEAB; 50 mM, dilution 1:4) and proteins were further digested with trypsin (3.75 ng μL^{-1}; sequencing grade, modified, Promega) at 37°C for 16 h. Samples were acidified to 1% v/v formic acid (FA; final pH ca. 2–3) and peptides were desalted and concentrated using Sep-Pak C18 1 cc Vac cartridges (Waters): The C18 material was pre-treated with MeCN (1 mL), H_2O_{dd}/0.5% TFA (1 mL), 80% MeCN/0.5% FA (1 mL) and H_2O_{dd}/0.1% TFA (2 mL) prior to sample loading. The beads were pelleted and the peptide solution was loaded to the cartridges. Peptides bound to the cartridges were washed with H_2O_{dd}/0.1% TFA (3 mL) and H_2O_{dd}/0.5% FA (1 mL) and eluted with 80% MeCN/0.5% FA (750 μL). The peptides were freeze-dried with a speedvac centrifuge.

LC-MS/MS analysis

Prior to mass spectrometry, peptides were reconstituted in 0.5% FA and filtered (0.22 μm PVDF filters; Millipore). Nanoflow LC-MS/MS analysis was performed with an UltiMate 3000 Nano HPLC system (Thermo Fisher Scientific) coupled to an Orbitrap Fusion (Thermo Fisher Scientific). Peptides were loaded on a trap column (Acclaim C18 PepMap100 75 μm ID× 2 cm; Thermo Fisher Scientific) and washed for 10 min with 0.1% FA, then transferred to an analytical column (Acclaim C18 PepMap RSLC, 75 μm ID×50 cm; Thermo Fisher Scientific) and separated using a 125 min gradient

from 5 to 32% (105 min from 5 to 22%, 10 min to 32% and 10 min to 90%) MeCN in 0.1% FA at a flow rate of 300 nL min^{-1}. Peptides were ionized using a nanospray source at 1.9 kV and a capillary temperature of 275 °C. Orbitrap Fusion was operated in a top speed data-dependent mode with a cycle time of 3 s. Full scan acquisition (scan range of 300–1700 m/z) was performed in the orbitrap at a resolution of 120 000 (at m/z 200) and with an automatic gain control ion target value of 4e5, maximum injection time set to 50 ms. Monoisotopic precursor selection as well as dynamic exclusion of 60 s were enabled. Internal calibration was performed using the ion signal of fluoranthene cations (EASY-ETD/IC source). Most intense precursors with charge states of 2–7 and intensities greater than 5e3 were selected for fragmentation. Isolation was performed in quadrupole using a window of 1.6 m/z. Ions were collected to a target of 1e4 for a maximum injection time of 40 ms with "inject ions for all available parallelizable time" enabled. Fragments were generated using higher-energy collisional dissociation (HCD) and detected in the ion trap at a rapid scan rate.

Protein identification and quantification

Peptide and protein identifications were performed using Max-Quant (v 1.5.2.0)[39] with Andromeda[40] as search engine with the following parameters: Carbamidomethylation of cysteines as fixed and oxidation of methionine as well as acetylation of protein N-termini as dynamic modifications; trypsin and LysC as the proteolytic enzymes with two missed cleavages allowed; 4.5 ppm for precursor mass tolerance (main search ppm) and 0.5 Da for fragment mass tolerance (ITMS MS/MS tolerance). Searches were performed against the Uniprot database for Homo sapiens (taxon identifier: 9606, downloaded on 15.10.2018). Quantification of SILAC pairs was carried out based on unique peptides only using "Arg6" and "Lys4" as "light" and "Arg10" and "Lys8" as "heavy" isotope identifiers requiring a minimum ratio count of 2. "I=L" and "requantify" (default settings) options were used. For raw files resulting from label switched experiments, the isotope identifiers were defined in reverse order resulting in ratios probe vs. DMSO. The mass spectrometry proteomics data have been deposited with the ProteomeXchange Consortium via the PRIDE[41] partner repository (http://www.ebi.ac.uk/pride) with the dataset identifier PXD014175. For statistical analysis with Perseus (v 1.6.2.2),[42] MaxQuant result table "proteinGroups.txt" based on two biological replicates (forward SILAC+SILAC label switch) with three technical replicates each were used. Putative contaminants, reverse hits and only identified by site hits were removed. SILAC ratios were $\log_2$-transformed, hits with less than four valid values removed and $-\log_{10}$(p-values) were obtained by a two-sided one sample Student's t-test over six replicates. The processed tables for protein group analysis in Perseus have been uploaded to the Supporting Information as an Excel file (Supporting Table in the Supporting Information).

Conflict of interest

The authors declare no conflict of interest.

[1] D. J. Newman, G. M. Cragg, *J. Nat. Prod.* **2016**, *79*, 629.
[2] E. Patridge, P. Gareiss, M. S. Kinch, D. Hoyer, *Drug Discovery Today* **2016**, *21*, 204.
[3] M. Anchel, A. Hervey, W. J. Robbins, *Proc. Natl. Acad. Sci. USA* **1950**, *36*, 300.
[4] M. Anchel, A. Hervey, W. J. Robbins, *Proc. Natl. Acad. Sci. USA* **1952**, *38*, 927.
[5] H. Shirahama, Y. Fukuoka, T. Matsumoto, *Bull. Chem. Soc. Jpn.* **1962**, *35*, 1047.
[6] K. Nakanishi, M. Ohashi, M. Tada, Y. Yamada, *Tetrahedron* **1965**, *21*, 1231.
[7] T. Matsumoto, H. Shirahama, A. Ichihara, Y. Fukuoka, Y. Takahashi, Y. Mori, M. Watanabe, *Tetrahedron* **1965**, *21*, 2671.
[8] T. C. McMorris, M. Anchel, *J. Am. Chem. Soc.* **1963**, *85*, 831.
[9] M. J. Kelner, T. C. McMorris, W. T. Beck, J. M. Zamora, R. Taetle, *Cancer Res.* **1987**, *47*, 3.
[10] M. Tanasova, S. J. Sturla, *Chem. Rev.* **2012**, *112*, 3578.
[11] M. J. Kelner, T. C. McMorris, L. Estes, R. J. Starr, M. Rutherford, M. Montoya, K. M. Samson, R. Taetle, *Cancer Res.* **1995**, *55*, 4936.
[12] T. C. McMorris, M. J. Kelner, W. Wang, M. A. Diaz, L. A. Estes, R. Taetle, *Experientia* **1996**, *52*, 75.
[13] T. C. McMorris, M. J. Kelner, W. Wang, J. Yu, L. A. Estes, R. Taetle, *J. Nat. Prod.* **1996**, *59*, 896.
[14] R. Williams, *Expert Opin. Invest. Drugs* **2013**, *22*, 1627.
[15] J. Walser, P. F. Heinstein, *Antimicrob. Agents Chemother.* **1973**, *3*, 357.
[16] M. J. Kelner, T. C. McMorris, L. Estes, M. Rutherford, M. Montoya, J. Goldstein, K. Samson, R. Starr, R. Taetle, *Biochem. Pharmacol.* **1994**, *48*, 403.
[17] T. C. McMorris, M. J. Kelner, R. K. Chadha, J. S. Siegel, S. Moon, M. M. Moya, *Tetrahedron* **1989**, *45*, 5433.
[18] T. C. McMorris, M. J. Kelner, W. Wang, S. Moon, R. Taetle, *Chem. Res. Toxicol.* **1990**, *3*, 574.
[19] T. C. McMorris, M. J. Kelner, W. Wang, L. A. Estes, M. A. Montoya, R. Taetle, *J. Org. Chem.* **1992**, *57*, 6876.
[20] R. A. Dick, X. Yu, T. W. Kensler, *Clin. Cancer Res.* **2004**, *10*, 1492.
[21] J. Gong, V. G. Vaidyanathan, X. Yu, T. W. Kensler, L. A. Peterson, S. J. Sturla, *J. Am. Chem. Soc.* **2007**, *129*, 2101.
[22] K. Tanaka, T. Inoue, S. Kadota, T. Kikuchi, *Xenobiotica* **1990**, *20*, 671.
[23] K. Tanaka, T. Inoue, S. Kadota, T. Kikuchi, *Xenobiotica* **1992**, *22*, 33.
[24] K. E. Pietsch, P. M. Van Midwoud, P. W. Villalta, S. J. Sturla, *Chem. Res. Toxicol.* **2013**, *26*, 146.
[25] K. Tanaka, T. Inoue, Y. Tezuka, T. Kikuchi, *Xenobiotica* **1996**, *26*, 347.
[26] M. C. Herzig, B. Arnett, J. R. MacDonald, J. M. Woynarowski, *Biochem. Pharmacol.* **1999**, *58*, 217.
[27] X. Liu, S. J. Sturla, *Mol. Biosyst.* **2009**, *5*, 1013.
[28] X. Liu, K. E. Pietsch, S. J. Sturla, *Chem. Res. Toxicol.* **2011**, *24*, 726.
[29] T. Wirth, K. Schmuck, L. F. Tietze, S. A. Sieber, *Angew. Chem. Int. Ed.* **2012**, *51*, 2874; *Angew. Chem.* **2012**, *124*, 2928.
[30] F. R. Kinder, R.-M. Wang, W. E. Bauta, K. W. Bair, *Bioorg. Med. Chem. Lett.* **1996**, *6*, 1029.
[31] A. Arnone, L. Merlini, G. Nasini, O. Vajna de Pava, F. Zunino, *J. Chem. Soc. Perkin Trans. 1* **2001**, 610.
[32] R. Schobert, B. Biersack, S. Knauer, M. Ocker, *Bioorg. Med. Chem.* **2008**, *16*, 8592.
[33] R. Schobert, S. Knauer, S. Seibt, B. Biersack, *Curr. Med. Chem.* **2011**, *18*, 790.
[34] Z. Li, P. Hao, L. Li, C. Y. J. Tan, X. Cheng, G. Y. J. Chen, S. K. Sze, H. M. Shen, S. Q. Yao, *Angew. Chem. Int. Ed.* **2013**, *52*, 8551; *Angew. Chem.* **2013**, *125*, 8713.
[35] P. Kleiner, W. Heydenreuter, M. Stahl, V. S. Korotkov, S. A. Sieber, *Angew. Chem. Int. Ed.* **2017**, *56*, 1396; *Angew. Chem.* **2017**, *129*, 1417.
[36] R. Huisgen, *Angew. Chem. Int. Ed. Engl.* **1963**, *2*, 565; *Angew. Chem.* **1963**, *75*, 604.

[37] V. V. Rostovtsev, L. G. Green, V. V. Fokin, K. B. Sharpless, *Angew. Chem. Int. Ed.* **2002**, *41*, 2596; *Angew. Chem.* **2002**, *114*, 2708.

[38] C. W. Tornøe, C. Christensen, M. Meldal, *J. Org. Chem.* **2002**, *67*, 3057.

[39] J. Cox, M. Mann, *Nat. Biotechnol.* **2008**, *26*, 1367.

[40] J. Cox, N. Neuhauser, A. Michalski, R. A. Scheltema, J. V. Olsen, M. Mann, *J. Proteome Res.* **2011**, *10*, 1794.

[41] J. A. Vizcaíno, A. Csordas, N. del-Toro, J. A. Dianes, J. Griss, I. Lavidas, G. Mayer, Y. Perez-Riverol, F. Reisinger, T. Ternent, Q.-W. Xu, R. Wang, H. Hermjakob, *Nucleic Acids Res.* **2016**, *44*, D447.

[42] S. Tyanova, T. Temu, P. Sinitcyn, A. Carlson, M. Y. Hein, T. Geiger, M. Mann, J. Cox, *Nat. Methods* **2016**, *13*, 731.

www.chemeurj.org